Optimal Capacity Planning of Integrated Energy System Considering Seasonal Ammonia Storage and Coordinated Multi-Hydrogen Ammonia Production

Jiang Liu
School of Electrical Engineering and Automation
Wuhan University
Wuhan, China
liujiang0709@whu.edu.cn

Chengxi Liu
School of Electrical Engineering and Automation
Wuhan University
Wuhan, China
liuchengxi@whu.edu.cn

Wei Zhang
School of Electrical Engineering and Automation
University of Shanghai for Science and Technology
Shanghai, China
zw19830904@usst.edu.cn

***Abstract*—Integrated energy system (IES) dominated by coal-fired power generation face multiple challenges such as low renewable energy penetration, high carbon emissions, and supply-demand imbalances. To address these issues, an ammonia-coal co-firing strategy is adopted to reduce carbon emissions, while coordinated ammonia production using multi-hydrogen energy sources ensures stable ammonia supply, while seasonal ammonia storage (SAS) enables cross-seasonal energy complementarity and supply-demand balance, effectively addressing the aforementioned challenges. This paper proposes a bi-level optimal capacity planning for IES considering SAS and coordinated multi-hydrogen ammonia production. The upper-level model minimizes the annual operation, maintenance, and scheduling costs, whereas the lower-level model minimizes the low-carbon dispatch cost for typical days. The proposed model is solved using an improved genetic algorithm to determine the optimal system capacity configuration and low-carbon scheduling strategy. Case studies have demonstrated that the proposed approach enhances renewable energy utilization, reduces overall system costs, and significantly decreases carbon emissions.**

***Keywords*—seasonal ammonia storage, multi-hydrogen, optimal capacity planning, ammonia production, integrated energy system**

I. INTRODUCTION

In response to the energy crisis and other environmental challenges, the world is transitioning towards low-carbon and sustainable energy consumption [1]. Integrated energy system (IES) utilizes a coupled and complementary approach to integrate multiple energy forms such as electricity, heating, cooling, and gas, thereby promoting the low-carbon transformation of energy systems [2]. However, in the existing IES, thermal generation (TG) still serves as the main flexible power source. The over-reliance on TG has resulted in significant carbon emission challenges for IES [3].

In recent years, IES have utilized the power to gas (P2G) technology to convert surplus renewable energy into hydrogen through water electrolysis(EL), and then transform it into methane to replace fossil fuels [4]. In [5], TG is integrated with carbon capture and storage (CCS) technology to achieve the capture and utilization of carbon emissions during energy production. Ammonia, as a zero-carbon energy carrier, has advantages such as ease of liquefaction, high energy density, making it suitable for large-scale storage, transportation, and utilization [6]. Existing research indicates that the adoption of ammonia-coal co-firing technology in TG can effectively improve the power generation efficiency of TG and reduce carbon emissions in the system [7]. A synergistic operation strategy for wind turbines (WT), power to ammonia (P2A), combined heat and power (CHP), and TG was proposed in [8]. This strategy has increased the utilization rate of renewable energy and reduced the system's carbon emissions.

However, the current production of ammonia requires a significant amount of hydrogen. As noted in [9], electricity to hydrogen (E2H) production using renewable energy often fails to fully meet system demands. Consequently, gas to hydrogen (G2H) or fuel to hydrogen (F2H) processes are typically relied upon as supplementary sources. Introducing ammonia storage into the production system can effectively optimize the dynamic balance in the hydrogen-ammonia conversion process [10]. In [11], a multi-energy storage operation strategy suitable for energy systems was proposed, and its impact on system reliability was analyzed. In [12], a hybrid energy storage model incorporating electrical storage, thermal storage, and hydrogen storage was constructed to address the challenges of renewable energy fluctuations and varying user demands within energy system.

Despite the aforementioned research, there are still the following issues in energy storage capacity configuration within IES: 1) Existing research on ammonia energy has not fully considered the long-term storage characteristics of ammonia storage, which further limits the complementary advantages of energy supply and demand; 2) Current multi-energy storage studies have not addressed the capacity configuration of ammonia storage. The ammonia synthesis and utilization stages need to integrate ammonia storage and optimize its capacity configuration to achieve more reasonable allocation results.

To address the aforementioned issues, this paper proposes a bi-level optimal capacity planning approach for IES, considering seasonal ammonia storage (SAS) and coordinated multi-hydrogen ammonia production. The main contributions and innovations of this paper are as follows:

(1) A mechanism for the cooperative operation of ammonia energy "synthesis-utilization-storage" is proposed. along with TG ammonia co-firing operation strategy, and a SAS model is established to analyze its operational characteristics in detail.

(2) A bi-level optimization model for multi-energy storage capacity allocation incorporating SAS has been proposed. This model considers both long term energy storage capacity configuration and short term low-carbon scheduling, further exploring the impact of ammonia storage configuration on various costs and carbon emissions.

XXX-X-XXXX-XXXX-X/XX/$XX.00 ©20XX IEEE
979-8-3315-8138-1

The rest of this paper is organized as follows. Section II develops a schematic and mathematical model of IES. Section III proposes a bi-level capacity configuration optimization strategy. Section IV validates the effectiveness of the proposed strategy. Finally, Section V presents the conclusions.

II. The Schematic and Mathematical Model of IES

A. The Schematic of IES

The framework of the IES is illustrated in Fig.1, consisting of four primary components: the power distribution network (PDN), heat distribution network (HDN), gas distribution network (GDN), and hydrogen distribution system (HDS). The carbon capture power plant (CCPP) consists of a CCS and a TG, gas is supplied from gas wells (GW) and undergoes gas to power conversion through gas turbines (GT) and CHP . The CHP, in conjunction with electric boilers (EB), collectively satisfies the system's thermal load requirements. Hydrogen supply is provided by blue hydrogen plant (BHP), hydrogen through EL, and grey hydrogen plant (GHP). The produced hydrogen reacts with nitrogen obtained through pressure swing adsorption (PSA) in ammonia plant (AP) to generate ammonia, which is utilized for co-firing in TG. the system is equipped with multiple energy storage facilities, including electric storage (ES), thermal storage (TS), hydrogen storage (HS), and ammonia storage (AS). Among these, AS can serve as a short-term or seasonal storage solution.

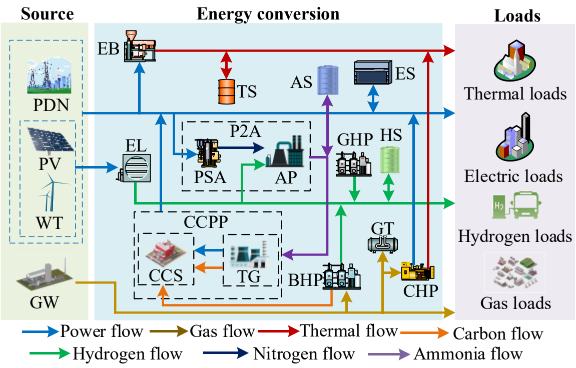

Fig. 1. Framework diagram of IES.

B. Multi-Hydrogen Energy Coordinated Ammonia Synthesis Framework

According to Fig. 2, the EL produces hydrogen by electrolyzing water through electrical energy supplied by the PDN, the generated hydrogen is distributed between the HS system and AP unit [9].

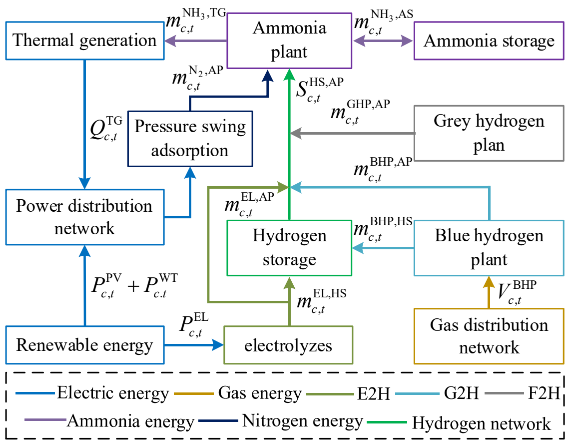

Fig. 2. Multi-hydrogen coordinated ammonia synthesis.

$$\begin{cases} m_{c,t}^{\mathrm{EL,HS}} + m_{c,t}^{\mathrm{EL,AP}} = P_{c,t}^{\mathrm{EL}} \eta_{\mathrm{EL}} / \mathrm{HHV} \\ P_{c,t}^{\mathrm{EL}} = P_{c,t}^{\mathrm{PV}} + P_{c,t}^{\mathrm{WT}} \end{cases} \tag{1}$$

where $m_{c,t}^{\mathrm{EL,HS}}$ denotes the hydrogen energy content stored in HS from EL output; $m_{c,t}^{\mathrm{EL,AP}}$ denotes the hydrogen energy utilized by AP from EL production; $P_{c,t}^{\mathrm{EL}}$ denotes the electrical energy input to the EL system; HHV denotes the higher heating value of hydrogen; $P_{c,t}^{\mathrm{PV}}$ denotes PV generation allocated to EL operation; and $P_{c,t}^{\mathrm{WT}}$ denotes WT power supplied to EL.

The model of AP can be represented as follows:

$$\begin{cases} m_t^{\mathrm{N_2}} = (P_t^{\mathrm{WT,PSA}} + P_t^{\mathrm{PV,PSA}} + P_t^{\mathrm{PG,PSA}}) / w_{\mathrm{N_2}} \\ m_t^{\mathrm{NH_3,AP}} = \mu_{\mathrm{H_2}}^{\mathrm{NH_3}} m_t^{\mathrm{H_2,AP}} + \mu_{\mathrm{N_2}}^{\mathrm{NH_3}} m_t^{\mathrm{N_2,AP}} \\ m_t^{\mathrm{AP}} = \lambda^{\mathrm{AP}} m_t^{\mathrm{NH_3,in}} \\ m^{\mathrm{AP,min}} \le m_t^{\mathrm{AP}} \le m^{\mathrm{AP,max}} \end{cases} \tag{2}$$

where $m_t^{\mathrm{N_2}}$ denotes the nitrogen energy at time t; $w_{\mathrm{N_2}}$ denotes the specific energy requirement for nitrogen-based energy generation, expressed in energy units per mass unit; $m_t^{\mathrm{NH_3,AP}}$ is the ammonia production of the AP; $m_t^{\mathrm{H_2,AP}}$ denotes hydrogen energy utilization rate within system AP at time t; $m_t^{\mathrm{N_2,AP}}$ denotes the nitrogen energy consumed by the AP at time t; $\mu_{\mathrm{H_2}}^{\mathrm{NH_3}}$ and $\mu_{\mathrm{N_2}}^{\mathrm{NH_3}}$ respectively denote the hydrogen-to-ammonia and nitrogen-to-ammonia energy conversion ratios in the synthesis process; λ^{AP} denotes the ammonia production efficiency in the Haber-Bosch process (AP); $m^{\mathrm{AP,max}}$ and $m^{\mathrm{AP,min}}$ denote the maximum and minimum ammonia production of the AP.

The AP system's hydrogen supply is sourced through multiple pathways: EL production, HS discharge, and methane reforming processes in both BHP and GHP, and can be expressed as:

$$\sum_{\mathrm{EL,BHP,HS,GHP} \in i} \left(m_{c,t}^{\mathrm{EL,AP}} + m_{c,t}^{\mathrm{HS,\,AP}} + S_{c,t}^{\mathrm{BHP,\,AP}} + m_{c,t}^{\mathrm{GHP,AP}} \right) = m_{i,t}^{\mathrm{H_2,AP}} \tag{3}$$

$$m_t^{\mathrm{NH_3,TG}} + m_t^{\mathrm{NH_3,AS}} = m_t^{\mathrm{NH_3,AP}} \tag{4}$$

where $m_{c,t}^{\mathrm{GHP,AP}}$ denotes the hydrogen energy output from the GHP; while $m_{i,t}^{\mathrm{H_2,AP}}$ denotes the hydrogen energy input to the AP; $m_t^{\mathrm{NH_3,TG}}$ denotes the ammonia doping of TG at time t; $m_t^{\mathrm{NH_3,AS}}$ denotes the ammonia storage energy at time t.

C. Model of Seasonal Ammonia Storage

According to Fig. 3, The operational constraints for SAS mode can be expressed as follows [13]:

$$\begin{cases} 0 \le P_{st}^{\mathrm{SAS+}} \le \varepsilon_{st}^{\mathrm{SAS+}} \tau^{\mathrm{SAS}} x^{\mathrm{SAS}} W^{\mathrm{SAS}} \\ 0 \le P_{st}^{\mathrm{SAS-}} \le \varepsilon_{st}^{\mathrm{SAS-}} \tau^{\mathrm{SAS}} x^{\mathrm{SAS}} W^{\mathrm{SAS}} \end{cases} \tag{5}$$

where $P_{st}^{\mathrm{SAS+}}$ and $P_{st}^{\mathrm{SAS-}}$ denote the charge and discharge power, respectively; $\varepsilon_{st}^{\mathrm{SAS+}}$ and $\varepsilon_{st}^{\mathrm{SAS-}}$ denote binary variables (0-1) indicating the charge and discharge states; τ^{SAS} denotes the power-to-capacity ratio of the SAS; x^{SAS} denotes whether SAS is installed; and W^{SAS} denotes the configured capacity of SAS.

$$\begin{cases} S_{s,0}^{\mathrm{SAS}} = (1 - \gamma_{loss}^{\mathrm{SAS}} D_0 w(s-1)\Delta t) \\ \qquad \times (S_{s-1,0}^{\mathrm{SAS}} + D_0 w(s-1) \\ \qquad \times (S_{s-1,24}^{\mathrm{SAS}} - S_{s-1,0}^{\mathrm{SAS}})) \\ S_{s,t}^{\mathrm{SAS}} = (1 - \gamma_{loss}^{\mathrm{SAS}}) S_{s,t-1}^{\mathrm{SAS}} \\ \qquad + (P_{s,t}^{\mathrm{SAS+}} \eta^{\mathrm{LAS+}} - P_{s,t}^{\mathrm{SAS-}} / \eta^{\mathrm{SAS-}}) \Delta t \end{cases} \tag{6}$$

979-8-3315-8138-1

$$\begin{cases} S_{1,0}^{\text{SAS}} = S_{N_s,24}^{\text{SAS}} \\ \varepsilon_{st}^{\text{SAS+}} + \varepsilon_{st}^{\text{SAS-}} \le 1 \end{cases} \tag{7}$$

where D_0 denotes the number of days in one year; $w(s)$ denotes the probability of typical day s; and $\gamma_{loss}^{\text{SAS}}$ is the self-discharge rate. The initial value of S is the cumulative value of the previous season's charge/discharge power minus the energy loss caused by self-discharge. (7) indicates that the final energy storage value equals the initial energy storage value, with a cycle duration of 8760 hours.

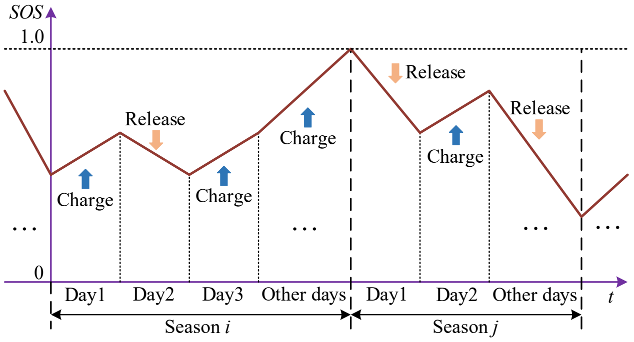

Fig. 3. Seasonal ammonia storage schematic diagram.

III. Bi-Level Capacity Configuration Optimization Strategy

The temporal difference between multi-energy storage capacity planning and low-carbon dispatch is taken into account. a bi-level collaborative optimization model was conducted to evaluate the synergistic effects between annual storage capacity configuration and daily operational dispatch.

A. Upper-Level Capacity Configuration Optimization Model

The upper-level model has the objective of minimizing the operation and maintenance cost of each type of energy storage equipment and the system operation cost. The objective function is shown in (8).

$$\min C_{\text{total}} = C_{\text{inv}} + C_{\text{main}} + \sum_{d=1}^{365} C_{\text{OC}} \tag{8}$$

where C_{inv} denotes the investment cost of the energy storage device; C_{main} denotes the annual maintenance cost of the energy storage device; C_{OC} denotes the total daily operating cost of the system, and d denotes the number of days.

The remaining items are costed as follows:

$$\begin{cases} C_{\text{inv}} = (\sum_{S\in\Omega_S} C_S T_{S,\text{N}}) \dfrac{r(1+r)^{Y_S}}{(1+r)^{Y_S}-1} \\ \Omega_S = \{\text{ES,TS,HS,AS}\} \end{cases} \tag{9}$$

$$C_{\text{main}} = \sum_{S\in\Omega_S} C_{\text{main},S} T_{S,\text{N}} \tag{10}$$

where Ω_S denotes the set of storage devices; C_S denotes the investment cost per unit capacity of energy storage S; $T_{S,\text{N}}$ denotes the planning capacity of device S; and Y_S denotes the operating life of energy storage S; $C_{\text{mian},S}$ denotes the annual maintenance cost per unit capacity of the energy storage S.

B. Lower-Level Low Carbon Dispatch Optimization Model

In order to achieve low carbon operation of the IES, the objective function is shown in (11) with the goal of minimizing the total operating cost of the IES on a typical day.

$$\min C_{\text{OC}} = C_{\text{EP}} + C_{\text{SCT}} + C_{\text{CCPP}} + C_{\text{CD}} + C_{\text{F2H}} + C_{\text{CA}} \tag{11}$$

where C_{EP} denotes the cost of energy purchase; C_{SCT} denotes the cost of carbon trading; C_{CCPP} denotes the cost of electricity generation in a CCPP; C_{CD} denotes the operational expenditures for the system; C_{F2H} denotes the specific production costs associated with F2H synthesis; C_{CA} denotes the cost of abandoned WT and PV.

C. Model Solution Process

The bi-level collaborative optimization model proposed in this paper is solved using an improved genetic algorithm. Its specific solution process comprises the following steps: 1) Fundamental parameters including the capacity boundaries of multi-energy storage are input as initial data; 2) An initial population is generated based on the capacity ranges of multi-energy storage devices, where each individual represents a distinct capacity configuration scheme; 3) Each population individual is evaluated through the lower-level low-carbon dispatch model, with the objective function values computed using the Gurobi solver. The results are subsequently transmitted to the upper-level for processing, where fast non-dominated sorting thereby generating the first offspring population; 4) New offspring populations are generated through fundamental genetic algorithm operations including selection, crossover, and mutation; 5) The steps are iteratively executed until the maximum iteration count is reached, the optimal multi-energy storage capacity configuration and low-carbon operational scheme are output.

IV. Case Studies

A. System Description

To verify the reliability and effectiveness of the proposed seasonal ammonia storage and multi-hydrogen energy coordinated ammonia production model. The selected regional structure is shown in Fig. 1. Optimization planning is conducted using representative days from summer, winter, and transitional seasons. Fig. 4 and Fig. 5 illustrate the renewable energy generation curve and load curve for different typical days, respectively. The relevant parameters of the IES system are detailed in [14]-[15], where the renewable energy curtailment penalty coefficient is set at 0.2$/kWh. The case studies were validated on a computing platform equipped with an Intel Core i7 processor (1.61 GHz) and 32 GB of memory, utilizing the Gurobi solver within the MATLAB 2021a environment.

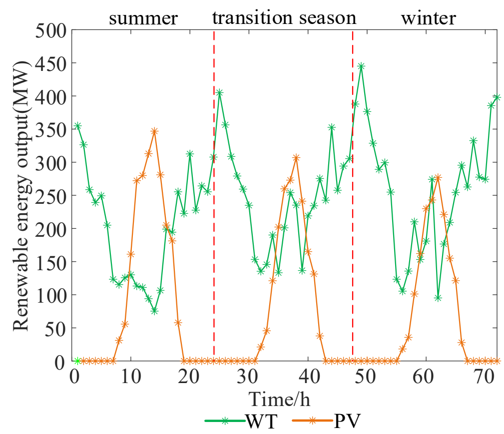

Fig. 4. Renewable energy generation curves for different typical days.

979-8-3315-8138-1

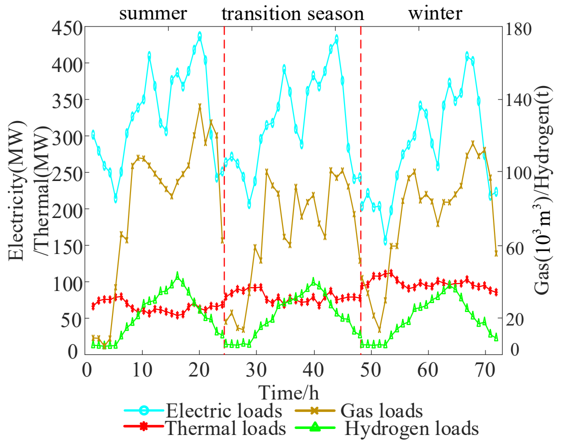

Fig. 5. Load curves for different typical days.

B. *Capacity Configuration Results Analysis*

To compare with existing optimization strategies, this paper compared four-group of cases. The optimization methods are shown in Table I.

TABLE I. OPTIMIZATION METHODS OF CASES.

Case	Multi-Hydrogen	Capacity configuration	SAS
1	×	√	×
2	√	√	×
3	√	√	√

TABLE II. SYSTEM TOTAL COST AND ENERGY STORAGE CAPACITY CONFIGURATION RESULTS UNDER DIFFERENT CASES.

	Case	Case1	Case2	Case3
Cost/10^4\$	Investment costs	1672.88	1437.78	1393.62
	Maintenance costs	536.60	428.33	405.73
	Operating cost	2351.07	2269.74	2212.43
	Total costs	4560.55	4135.85	4011.78
Configuration capacity	ES/MWh	250	200	200
	TS/MWh	50	45	45
	HS/t	8.12	6.24	5.83
	AS/t	0	2.97	3.26

As shown in Table II, Case 3 has hydrogen storage capacities and ammonia storage capacities of 4.83 tons and 3.42 tons, respectively. Compared to Case 2, this represents a 6.57% reduction in hydrogen storage capacity and a 9.76% increase in ammonia storage capacity. These results indicate that seasonal ammonia storage requires higher ammonia demand on typical days, thereby increasing the hydrogen to ammonia conversion process to reserve more ammonia energy. Since both Case 2 and Case 3 have lower investment and operating costs than Case 1, their total costs are also lower than Case 1. Specifically, the total cost of Case 3 is reduced by 12.03% compared to Case 1. Thus, the proposed optimal configuration model reduces the system's total cost by 12.03% through rational planning of energy storage investment and optimized operation.

C. *System Low Carbon Scheduling Analysis*

Fig. 6 illustrates the hourly carbon emissions from various internal processes of the system in Case 3 over a 24-hour period, providing a clear visualization of emissions generated during multi-source hydrogen coordinated ammonia production. Furthermore, the system prioritizes green ammonia, supplemented by blue ammonia, with gray ammonia serving as a backup. As illustrated in Fig. 7, when the carbon price growth rate increases from 0 to 0.4, carbon emissions are reduced by approximately 75t, while the system operational cost increases by about 7×10^3\$. This demonstrates that a higher carbon price growth rate promotes carbon emission reduction but also raises operational costs.

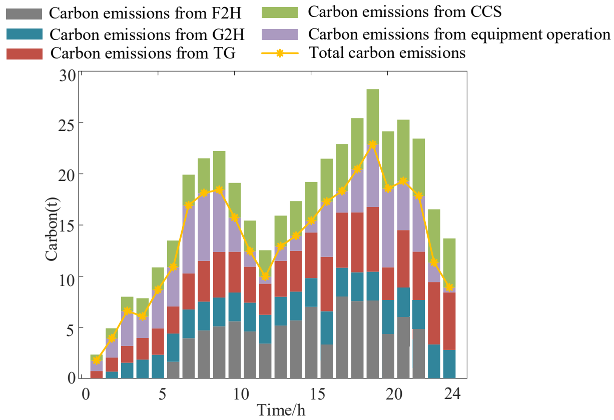

Fig. 6. Carbon emissions by process within the system in Case 3.

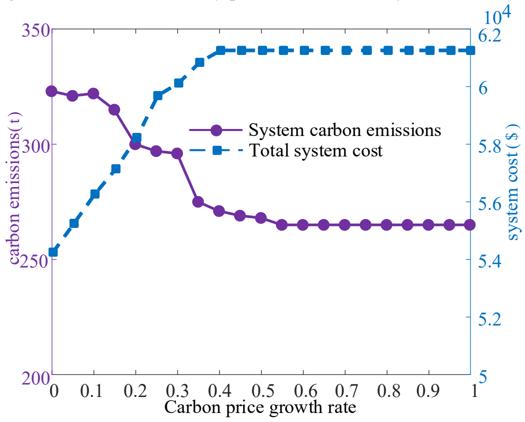

Fig. 7. The relationship between carbon price growth rate, carbon emissions, and total costs.

D. *Seasonal Ammonia Storage Benefit Analysis*

As shown in Fig. 8, Case 1 exhibits a higher surplus of wind and solar power, placing greater demands on the system to improve renewable energy consumption rates. With the introduction of ammonia co-firing, the ammonia production consumes a significant amount of hydrogen. In Case 3, the actual output of wind and solar power closely matches the forecasted output for most time. Compared to Case 1, during 0:00-6:00 and 23:00-24:00, abundant wind power and low energy demand facilitate the processes of E2H and PSA, thereby promoting the utilization rate of renewable energy.

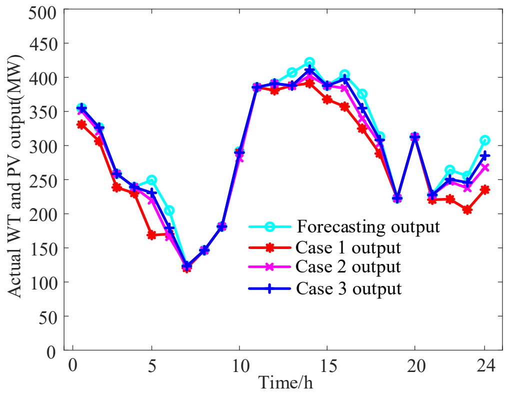

Fig. 8. Schematic diagram of renewable energy forecast under various cases.

979-8-3315-8138-1

As shown in Fig.9, during the 0:00-6:00 period on days with varying typical daily conditions, ammonia production significantly exceeds consumption due to higher renewable energy generation, enabling ammonia storage to accumulate surplus ammonia energy. During the 8:00-10:00 and 16:00-20:00 periods, when thermal power generation output is high, ammonia consumption exceeds production, necessitating the release of stored ammonia energy to meet demand. As shown in Fig. 10, on days 1 and 7, when ammonia consumption was low, the SAS system entered an energy storage state, releasing it during days 4 and 10 when usage is high. This demonstrates ammonia energy's role as a seasonal storage, enabling cross-period storage and release to achieve energy complementarity between different typical days.

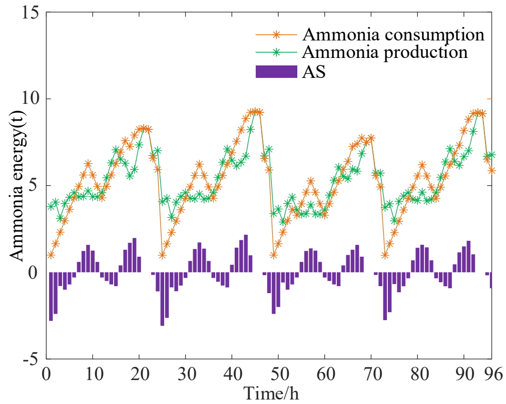

Fig. 9. Ammonia energy balance for short-term storage in Case 2.

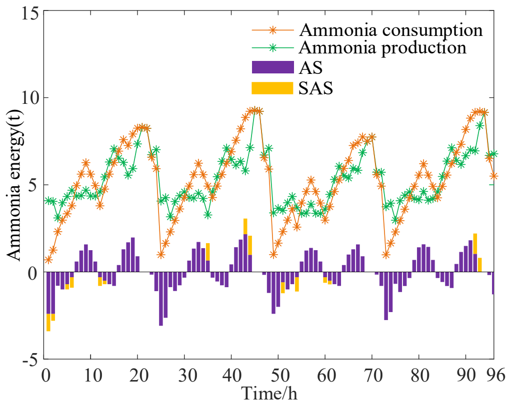

Fig. 10. Ammonia energy balance for seasonal storage in Case 3.

V. Conclusion

This paper proposes a bi-level collaborative optimization model is established for IES, considering multi-hydrogen-coordinated ammonia synthesis and multi-energy storage to address carbon emissions and economic challenges in IES. The main contributions and results are as follows:

(1) A mechanism for the cooperative operation of ammonia energy "synthesis-utilization-storage" meets system ammonia demand and promotes TG with ammonia co-combustion. The proposed framework facilitates emission reduction and optimized energy efficiency.

(2) By considering the coordinated capacity configuration of electricity-heat-hydrogen-ammonia storage in multi-hydrogen-coordinated ammonia production for coal-fired unit operation, optimizing ammonia synthesis and utilization, enhancing renewable energy absorption rate. The proposed model reduces IES economic costs by 12.03%.

(3) The utilization of SAS in multi-energy storage systems can reduce operational costs and lower carbon emissions during routine dispatch operations while enabling energy transfer across different time periods.

Future efforts will further explore the potential for converting offshore wind power into ammonia production while conducting research on ammonia energy related safety issues to achieve flexible energy management and dispatch.

References

[1] B. Lin and Z. Li, "Towards world's low carbon development: the role of clean energy," *Applied Energy*, vol. 307, pp. 118160, Feb. 2022.

[2] Y. Wang, J. Hu, and N. Liu, "Energy management in integrated energy system using energy-carbon integrated pricing method," *IEEE Transactions on Sustainable Energy*, vol. 14, no. 4, pp. 1992-2005, Oct. 2023.

[3] J. Jin, Q. Wen, S. Cheng, Y. Qiu, X. Zhang, and X. Guo, "Optimization of carbon emission reduction paths in the low-carbon power dispatching process," *Renewable Energy*, vol. 188, pp. 425-436, Apr. 2022.

[4] J. Yang, N. Zhang, Y. Cheng, C. Kang, and Q. Xia, "Modeling the operation mechanism of combined P2G and gas-fired plant with CO_2 recycling," *IEEE Transactions on Smart Grid*, vol. 10, no. 1, pp. 1111-1121, Jan. 2019.

[5] Y. Zhang, P. Sun, X. Ji, M. Yang, and P. Ye, "Low-carbon economic dispatch of integrated energy systems considering full-process carbon emission tracking and low carbon demand response," *IEEE Transactions on Network Science and Engineering*, vol. 11, no. 6, pp. 5417-5431, Dec. 2024.

[6] A. Sánchez, M. Rengel, and M. Martín, "A zero CO_2 emissions large ship fuelled by an ammonia-hydrogen blend: reaching the decarbonisation goals," *Energy conversion and management*, vol. 293, pp. 117497, Oct. 2023.

[7] A. Sánchez, E. Castellano, M. Martín, and P. Vega, "Evaluating ammonia as green fuel for power generation: A thermo-chemical perspective," *Applied Energy*, vol. 293, pp. 116956, Jul. 2021.

[8] L. Li, C. Ning, G. Pan, L. Zhang, W. Gu, and L. Zhao, "A risk-averse just-in-time scheme for learning-based operation of microgrids with coupled electricity-hydrogen-ammonia under uncertainties," *IEEE Transactions on Sustainable Energy*, vol. 16, no. 4, pp. 2621-2635, Oct. 2025.

[9] W. Zhang and J. Liu, "Low-carbon optimal dispatch of park integrated energy system considering coordinated ammonia production from multiple hydrogen energy," *Renewable Energy*, Vol. 237, part B, pp. 121712, Dec. 2024.

[10] B. Kong, Q. Zhang, and P. Daoutidis, "Real-time operation of a stand-alone microgrid with green ammonia storage," *IEEE Transactions on Control Systems Technology*, vol. 32, no. 4, pp. 1463-1470, Jul. 2024.

[11] Z. Chen, Z. Li, D. Lin, C. Xie, and Z. Wang, "Multi-time-sscale optimal scheduling of integrated energy system with electric-thermal-hydrogen hybrid energy storage under wind and solar uncertainties," *Journal of Modern Power Systems and Clean Energy*, vol. 13, no. 3, pp. 904-914, May. 2025.

[12] W. Huang, N. Zhang, J. Yang, Y. Wang, and C. Kang, "Optimal configuration planning of multi-energy systems considering distributed renewable energy," *IEEE Transactions on Smart Grid*, vol. 10, no. 2, pp. 1452-1464, Mar. 2019.

[13] G. Pan, W. Gu, Y. Lu, H. Qiu, S. Lu, and S. Yao, "Optimal planning for electricity-hydrogen integrated energy system considering power to hydrogen and heat and seasonal storage," *IEEE Transactions on Sustainable Energy*, vol. 11, no. 4, pp. 2662-2676, Oct. 2020.

[14] J. Zhang, X. Chang, Y. Xue, X. Bai, Z. Li, and P. Wang, "Optimal planning for electricity-gas-hydrogen integrated energy systems considering intertemporal long-term hydrogen storage and multiple Uncertainties," *IEEE Transactions on Power Systems*, vol. 40, no. 6, pp. 4660-4674, Nov. 2025.

[15] X. Wang, S. Wang, Q. Zhao, and Z. Lin, "Low-carbon coordinated operation of electric-heat-gas-hydrogen interconnected system and benchmark design considering multi-energy spatial and dynamic coupling," *Energy*, vol. 279, pp. 128042, Sep. 2023.